

Investigation of the abrasive wear behaviour of ZA-27 alloy and CuSn10 bronze

Hamdullah Çuvalcı · Hasan Serdar Çelik

Received: 20 October 2010 / Accepted: 12 February 2011 / Published online: 24 February 2011
© Springer Science+Business Media, LLC 2011

Abstract In this study, abrasive wear behaviours of ZA-27 alloy and CuSn10 bronze were investigated using a purpose-built wear tester. The ZA-27 alloy was produced by permanent mould casting. The abrasive SiC particles having 63 µm grit size was added to the lubricant oil. The wear rate and friction coefficient of alloys were determined at the different test conditions such as sliding distance, applied load, linear velocity and percentage SiC weight content. The wear surfaces of alloys were examined using SEM and EDS analysis. The results showed that the wear rate of alloys decreased with the increasing of applied load and increased with the increasing linear velocity and abrasive SiC content. It was found that the SiC particle fracture was an important mechanism determining the friction and the wear rate of alloys. CuSn10 bronze showed higher wear resistance than ZA-27 alloy under abrasive test conditions except at high linear velocities.

Introduction

The zinc–aluminium (ZA) family of casting alloys are gaining wide commercial importance as journal bearing material for high load and low speed applications. These alloys, most notably ZA-12 and ZA-27 are capable of replacing traditional bronze bearing at low cost [1]. It is concluded from the study of full size bearings that ZA-12 and ZA-27 have equivalent or superior bearing performance than bronze alloys, particularly C93200 (SAE 660) lead–tin bronze [2]. It was reported that the ZA alloys,

when compared to bronze, had better anti-frictional properties, better emergency running properties, better embeddability, lower coefficient of friction, longer wear life and lower cost [3].

The ZA-27 alloy which is an important member of the ZA family of alloys with a high strength is reported to have properties equivalent to those of aluminium alloys. Abundant availability, good bearing and mechanical properties such as wear resistance, anti-seizure properties, yield and tensile strengths scored in favour of extensive use of these alloys for bearing applications [4, 5]. Recently, the ZA-27 alloy has been substituted for conventional journal bearing materials in a wide range of industrial applications [6]. The journal bearings produced from these alloys have been used in earthmoving equipments, mining and milling machines, cable winches and compressors [7, 8].

The ZA-27 alloys and the bearings were also used in heavy and dusty environments such as underground machines, mining equipments, ore crushers and rock drills. The hard particles and oxides from these environments such as silicon dioxide, aluminium oxide and silicon carbide could move into the working surfaces of the bearings and they could lead to three body type abrasive wear on these surfaces. In the literature there is not enough information and limited study about abrasive type wear of ZA-27 alloy especially comparative with the bronzes. This article presents the results of an experimental study conducted to determine three body abrasive wear properties of ZA-27 alloy and compared to CuSn10 bronze. The alloys have been examined at varying applied load, sliding distance, linear velocity and percent abrasive content in the oil. The abrasive particles were added to an engine oil (SAE 30) to simulate lubrication oil containing hard abrasive particles in a bearing oil system.

H. Çuvalcı (✉) · H. S. Çelik
Metallurgy and Materials Engineering Department,
Karadeniz Technical University, Trabzon, Turkey
e-mail: hcuvalci@ktu.edu.tr

Experimental procedure

Material preparation

The melting process was carried out in the temperature controlled electrical crucible furnace for ZA-27 alloy. The melted alloy was then cast into steel mould which was designed in the form of rectangular prism having the cavity of $174 \times 34 \times 12$ mm dimensions. In order to prepare ZA-27 alloy, copper addition was supplied from an inter-metallic copper–aluminium master alloy (46.5% Al) which was prepared in the laboratory. The purities of metal used to prepare ZA-27 and master alloy was 99.99% for zinc and copper and 99.97% for aluminium and magnesium. ZA-27 alloy was produced by using permanent mould casting in the laboratory, whereas CuSn10 bronze was procured from a commercial source.

Microscopic studies

The sample taken from the alloy casting for microstructural studies was prepared using standard metallographic techniques and etched at 70 °C with 25% Nital etchant (25% nitric acid and 75% ethanol). Its micrograph was taken using an optical microscope. The abrasive SiC particle micrographs and typical samples of wear surfaces were examined by using a scanning electron microscopy (SEM, ZEISS EVO LS10).

Abrasive wear tests

The specimens used in the wear tests were machined in a milling machine as rectangular prism with the dimension of $7 \times 16 \times 14$ mm. The one end of specimen was deliberately curved by 70 mm radius to enable abrasive + oil mixture enter into contact region between disc and specimen. Before tests the specimen surfaces were grinded using 1200 number emery paper and then polished using alumina suspension to get approximately same surface roughness for all specimens. Three body abrasion tests were conducted on the samples using a block-on ring type wear tester which was specially adapted for this purpose. A schematic representation of the test apparatus is shown in Fig. 1. The bottle of abrasive–oil mixture was stirred using a mixer during test to enable homogeneous distribution of the particles in the oil. The disc having 60 mm diameter and 12 mm thickness was made of 4140 type alloy steel and which was hardened to 62 HRC. The specimens were loaded against the disc by a cantilever mechanism and the abrasive flow was continuously feed to the contact region between disc and specimen. The wear tester consists of a speed control unit, an electric motor having 3 kW power, journal, disc, specimen holder, loading arm, friction force

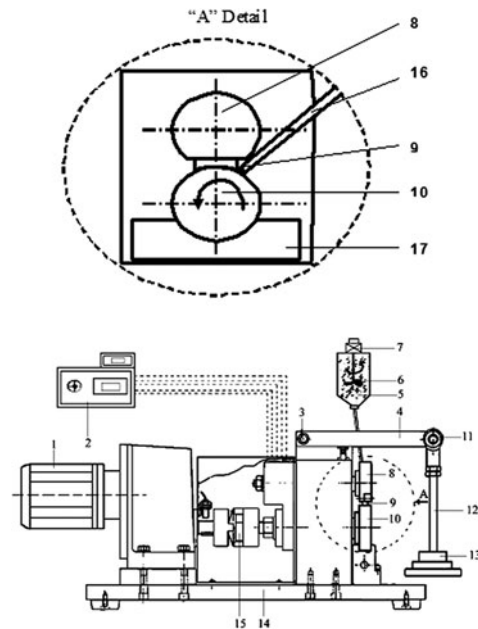


Fig. 1 A schematic representation of the block-on ring type wear tester. 1 Electronic motor, 2 control and data storage, 3 pin, 4 lever arm, 5 abrasive oil, 6 mixer, 7 mixer motor, 8 specimen holder, 9 specimen, 10 disc, 11 swivel joint, 12 hanger arm, 13 dead weights, 14 base table 15 clutch, 16 hose, 17 collecting case

measurement unit, data storage system and abrasive + oil mixture feeding system. The experiments were carried out for the forces of 30,60, 90,120 and 150 N, at the linear speeds of 0.31, 0.63, 0.94, 1.26 and 1.57 m/s. Moreover the sliding distance was changed of 55.8,111.6,167.4, 223.2 and 279 m (corresponding to 3, 6, 9, 12 and 15 min) and at the abrasive SiC ratio of 3, 6, 9 and 12 weight percent in the oil. The abrasive grit size was selected as $63 \mu\text{m}$ (+230 mesh size) for all these experiments. The flow rate of abrasive + oil mixture was 60 mL/min during all the tests. The specimen remained unchanged throughout the entire range of tests and fresh abrasive were used in the experiments. The working time between two data points was selected as 3 min (50.8 m) for all tests. The specimens were cleaned well with trichloroethylene in an ultrasonic cleaner and weighed before and after the wear tests using a microbalance. Each data point on the figures represents an average of three wear specimens. The friction force between disc and specimen was recorded using a measurement unit during the tests. The unit consist of a load-cell, a strain-indicator and a data-logger. The average friction coefficient was calculated using $\mu = F_s/F_n$ equation, where F_s is friction force and F_n is normal force.

The hardness of the alloys were determined by Brinell testing method using applied load as 31.25 kg and a ball indenter having 2.5 mm diameter.

Results and discussion

Figure 2a represent the microstructure of ZA-27 alloy at the casted condition. The alloy shows typical fine cored dendritic structures (α aluminium rich phase white areas) surrounded by a mixture of eutectoid reaction products $\alpha + \eta$ phases in which η is the zinc rich phase. Copper containing ϵ phase (CuZn_4) was found in the zinc rich η phase (white regions) as black irregular particles using SEM EDS analysis, Fig. 2b. The appearance of abrasive SiC particles is shown in Fig. 3. As seen from the figure that the SiC particles have angular form with sharp edges and corners.

The wear surfaces of alloys were examined using a stereo microscope and SEM. The macrographs of the worn surfaces of alloys were taken with stereo microscope are shown in Fig. 4a, b for Za-27 and bronze, respectively. Worn specimen surfaces can be divided into three regions. The first one is on the right hand side unworn small area showing little wear tracks which SiC particles enter from

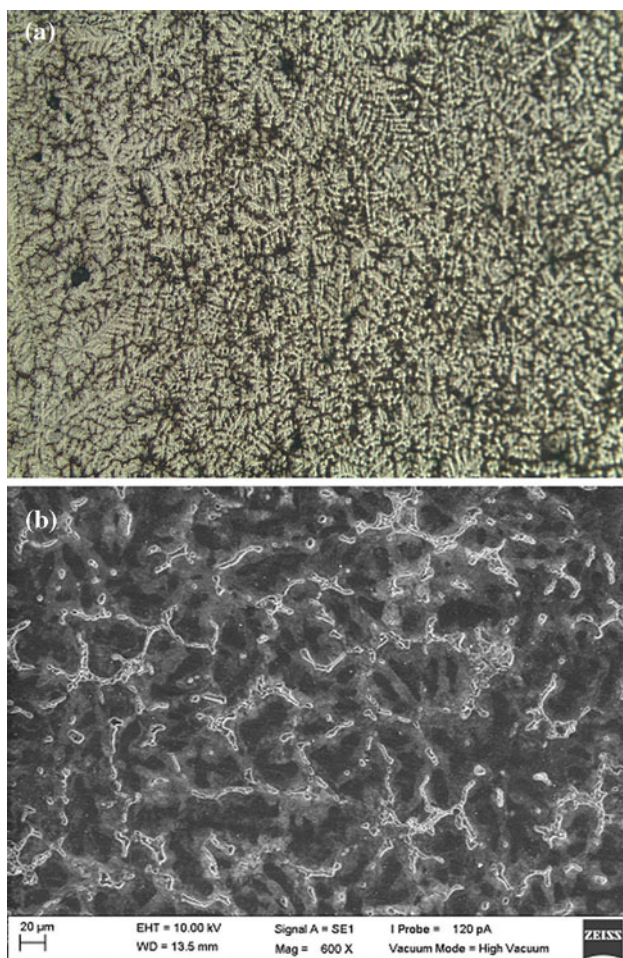


Fig. 2 The microstructures of ZA-27 alloy. **a** Optical microscope $\times 100$ and **b** SEM $\times 600$

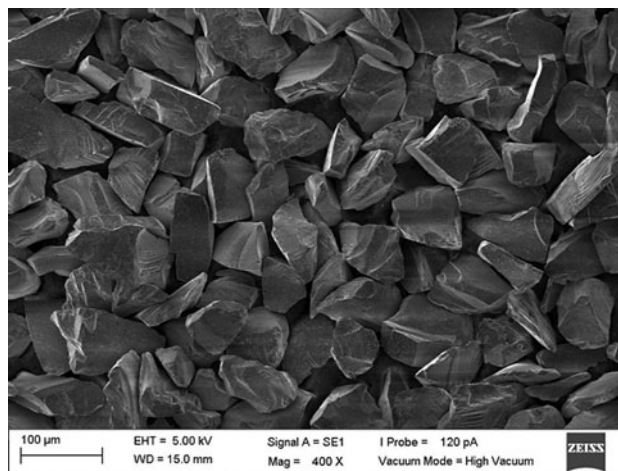


Fig. 3 Morphology of abrasive SiC particles

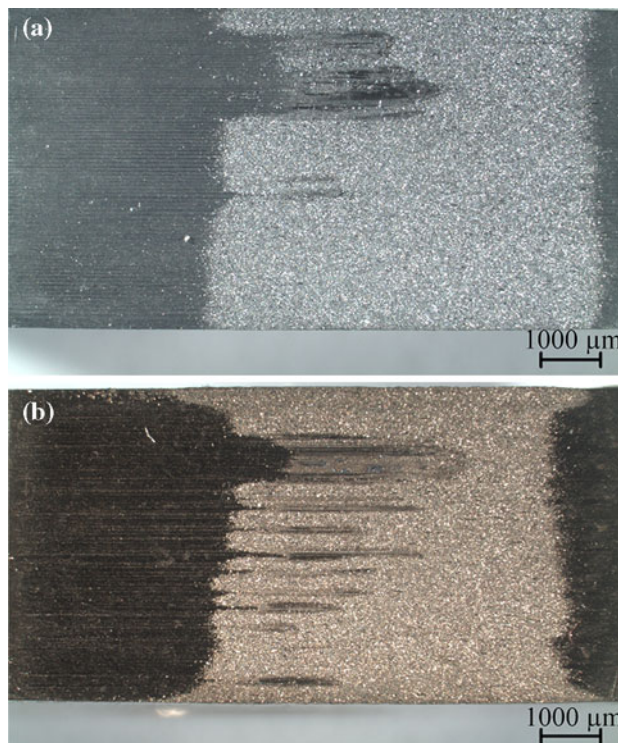


Fig. 4 Wear surfaces of alloys at 60 N, 0.31 m/s, 10% SiC and 279 m. **a** ZA-27 and **b** bronze

this side into the surface. In this part of the specimen there is no appreciable wear signs. At the middle of the specimen there is a wide region which shows worn areas and extensive embedded SiC particles into the surface. On the left hand side of specimens there is wide unworn regions in which the abrasive particles exit from specimen. Some wear furrows was observed on the middle region of both specimen along the direction of sliding. It can be seen from the figures that the alloys show same wear scar in the

middle part of the specimens but ZA-27 alloys exhibit more worn area than bronze for 279 m sliding distance. It was found that the main wear scar occurs in the central region of the specimens. This was due to the dimension difference between the specimen and the rotating disc. The disc radius was 30 mm whilst the specimen contact radius was 70 mm.

The SEM images of wear surfaces are shown in Fig. 5a, b for ZA-27 and bronze, respectively. The images show extensive and multi-directional microcutting and ploughing wear marks with debris smearing on the surfaces. On the other hand EDS analysis of ZA-27 alloy wear surface reveals big Si element peaks which indicate embedded SiC particles on the wear surfaces, Fig. 6. Figure 7a shows the embedded particles at the SEM image as small and more rounded ones than fresh abrasives for ZA-27 wear sample. These embedded particles were observed on the both alloy wear surfaces. The size of embedded particles are mostly in the range of 2–5 μm at low speed (0.31 m/s), although the some which are smaller than these, can be seen on the image. The high magnification of these SiC particles is

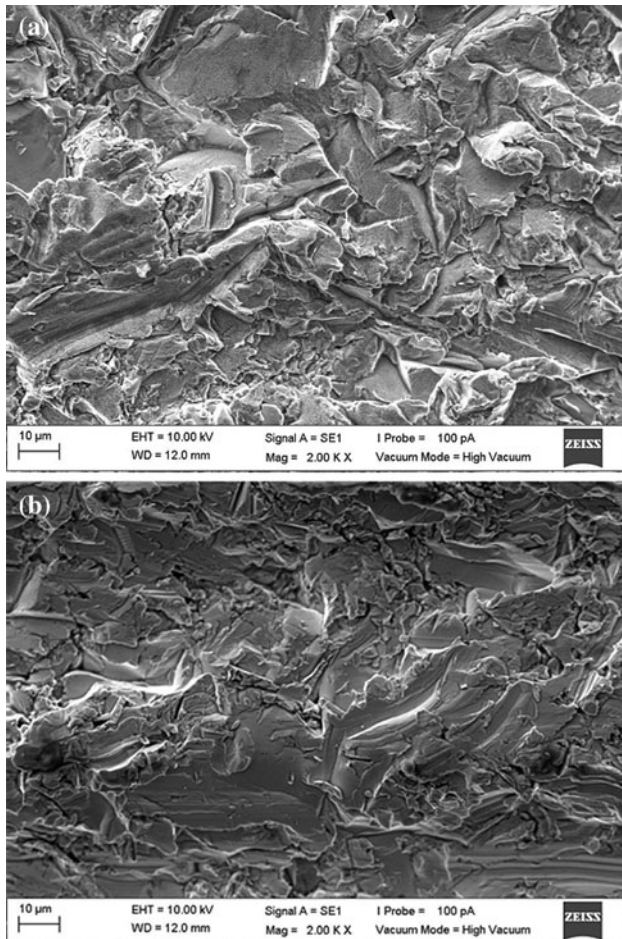


Fig. 5 SEM images of the wear surfaces. a ZA-27 and b bronze

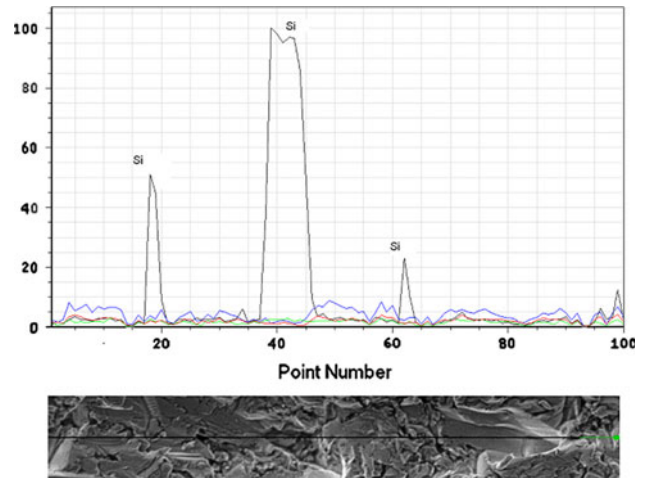


Fig. 6 EDS analysis of wear surface on the ZA-27 alloy

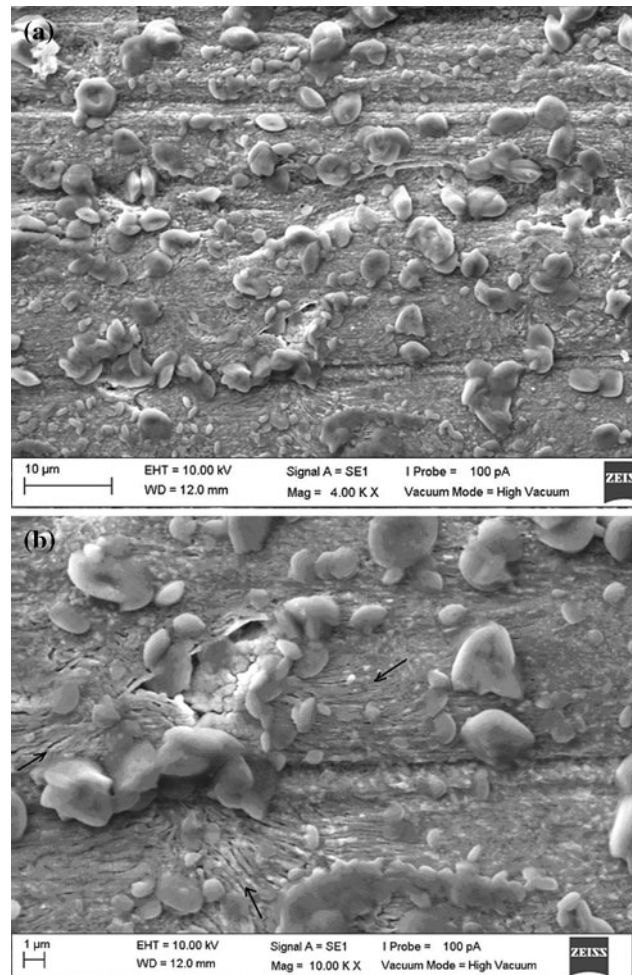


Fig. 7 Abrasive SiC particles embedded on the wear surfaces of ZA-27 alloy at 60 N, 0.31 m/s and 279 m. a ×4,000 and b ×10,000

given in Fig. 7b. This image also shows that the plastic deformation marks around the SiC particles as shown by arrows. The SiC particles on the wear surfaces are smaller

(2–5 μm) than the fresh abrasives having particle size of 63 μm . This reveals that the particles are subjected to the fragmentation process between disc and specimen during rubbing. In addition to that the particles seem to be more round and circular than the original ones. The EDS analysis reveals that the outer regions of the particles are surrounded with the wear debris such as Zn–Al or Cu–Sn elements. The particle fragmentation between rubbing surfaces has been noted by other authors [9].

The wear surface of bronze specimen at a linear speed of 1.57 m/s is given in Fig. 8. The wear tracks seem to be more heavier than the other wear surfaces having low linear speed such as 0.31 m/s in Fig. 5. Figure 8 also shows a single SiC particles as ploughing the surface and a huge wear track above this particle. The wear surface images of alloys at the 150 N load and 12% SiC are given in Figs. 9 and 10, respectively. These micrographs show wear signs such as indentation, grooves and scratches. It can be concluded that the abrasive particles have the freedom to roll and slide between the tested specimen and the rotating steel disc. The abrasive particles also have the chance to roll more than to slide, therefore the predominant wear mechanism is plastic deformation due to multi-indentations localized small grooves and fine scratches can also be observed due to sliding motion of the abrading particles.

The abrasive wear rates of the ZA-27 alloy and bronze versus sliding distance are shown in Fig. 11. From the figure it can be easily seen that the wear rate of both specimens increased at the beginning of the test. After reaching a maximum point the wear rates decreased with sliding distance. Maximum wear rate was observed at the sliding distance of 100 m for ZA-27 alloy whereas that of bronze was observed at the sliding distance of 200 m. At the end of the test over the entire sliding distance (279 m) ZA-27 alloy showed higher wear rate than

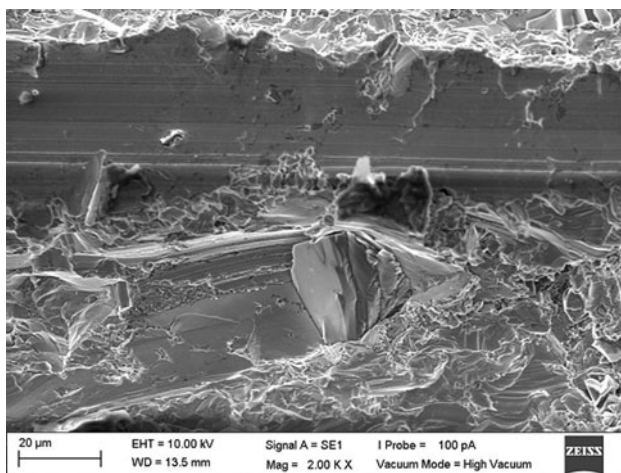


Fig. 8 Wear surface of bronze at 60 N, 1.57 m/s and 279 m

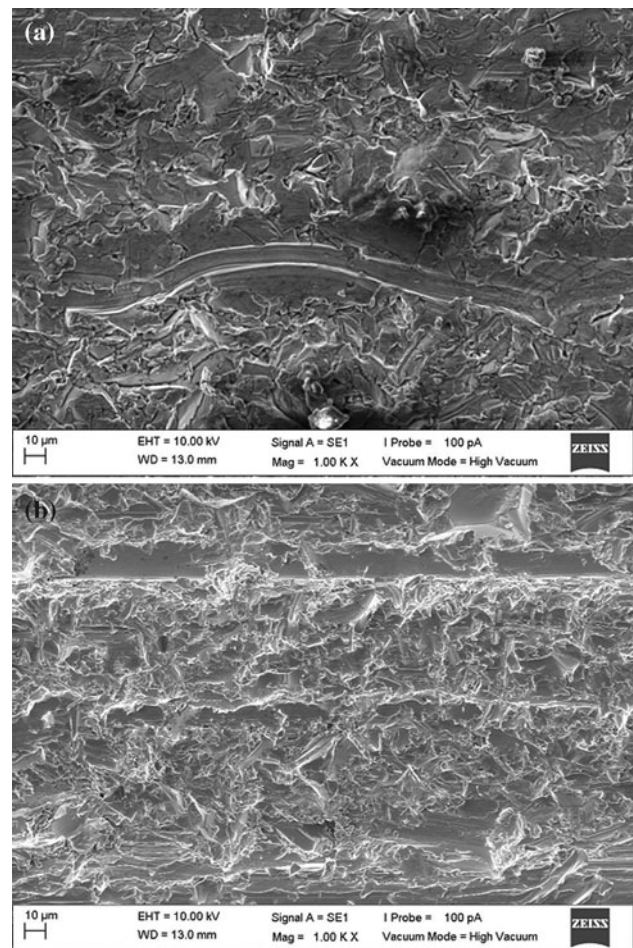


Fig. 9 Wear surfaces of alloys in SEM images at the load of 150 N ($\times 1000$), 0.31 m/s, 279 m and 10% SiC. **a** ZA-27 and **b** bronze

bronze. At the beginning of the test the surface was virgin and the abrasive effects of the particles on the surface wear were dominant. After reaching a maximum point for two alloys the wear rate began decreasing. This decreasing could be attributed to the frictional layer built up on the rubbing surface and the work hardening of the surface beneath which they can reduce the wear rate with sliding time [10]. A thin stable layer formed on the contacting surface of the specimen reduces the extent of direct contact of abrasive with the bulk of the material [11]. As long as the layer is stable and remains in contact with the specimen surface, the good wear resistance is displayed. However, whenever the layer disintegrates and the fresh bulk material comes into contact with the abrasive, the higher wear rate is experienced.

The variations of the abrasive wear rates of the alloys with the applied load are shown in Fig. 12. From this figure it is seen that the wear rates of the alloys decrease with the increasing load. As clearly seen from the figure that bronze showed higher wear resistance than ZA-27 alloy. At the

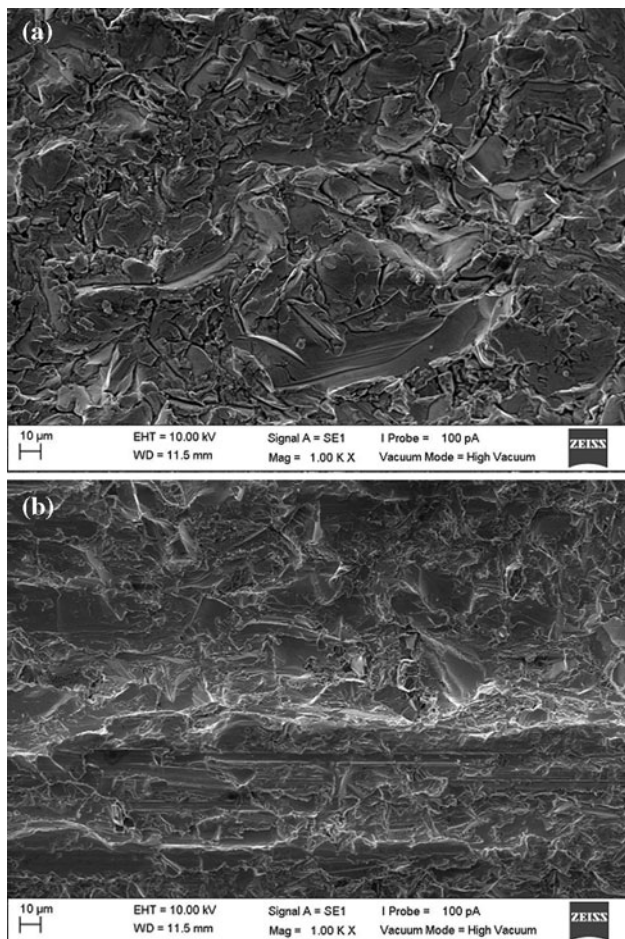


Fig. 10 Wear surfaces of alloys in SEM images at the 12% SiC content ($\times 1000$), 0.31 m/s, 60 N and 279 m/s. **a** ZA-27 and **b** bronze

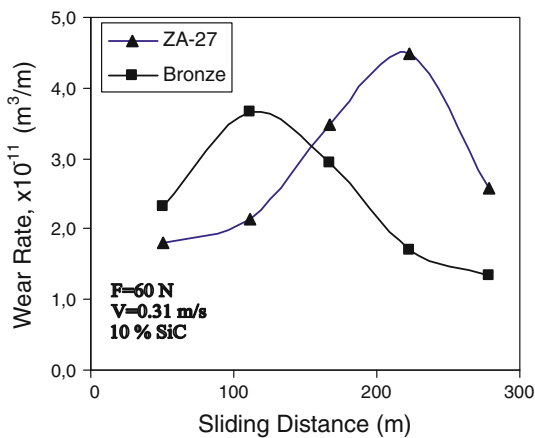


Fig. 11 Wear rate of specimens as a function of sliding distance

sliding distance of 279 m bronze showed the wear rate of $2.83 \times 10^{-11}(\text{m}^3/\text{m})$ whereas it was 3.57^{-11} for ZA-27 alloy. It was found that the wear rates of alloys decreased with the increasing of applied load, Fig. 12. This is an interesting result. This behaviour could be explained with

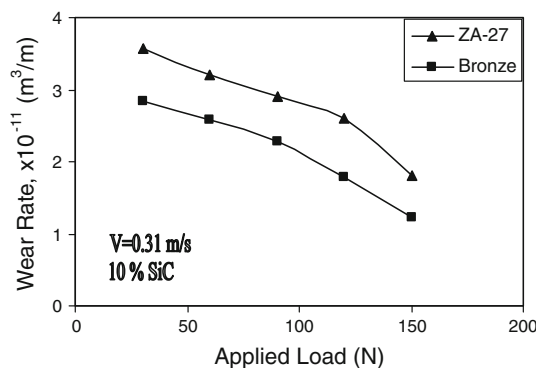


Fig. 12 Wear rate of specimens as a function of applied load

the test condition of specimen. Test condition involved conducting the abrasion tests using the fresh abrasive whilst the specimen surface remained unchanged (preworn) over the entire range of sliding distance, 279 m. As stated above the frictional layer and work hardening take place on the specimen surface along the sliding time. On the other hand the abrasive particle fragmentation and thus fine abrasives occur more easily at the higher applied load. This result is a good agreement with the study of Dube et al. [9]. They have shown that significant fracture of particles was observed in the high stress abrasion tests with increasing applied load. Fine abrasive particles due to particle fracture gives low wear and low friction. This result is in a good agreement with the study of Al-Rubaie et al. [12].

The effect of the linear velocity on the wear behaviour of alloys is shown in Fig. 13. The wear rates of alloy increased with the increasing linear velocity. At low velocity (0.31 m/s) the wear rates of alloy are $1.23^{-11} (\text{m}^3/\text{m})$ and 2.38^{-11} whereas at the high velocity (1.67 m/s) these values increase up to $7.28^{-11} (\text{m}^3/\text{m})$ and 41.9^{-11} for ZA-27 and bronze, respectively. As seen in Fig. 13, the bronze showed higher wear rate than that of ZA-27 alloy. It can be said that the linear velocity has great effect on the wear behaviour of alloys. This may be due to embedded SiC particle size on the rubbing surface. In Fig. 7a, the

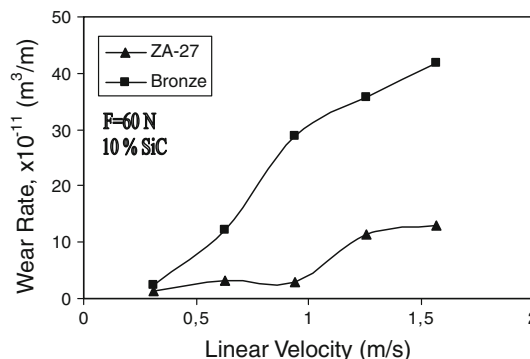


Fig. 13 Wear rate of specimens as a function of linear velocity

embedded particles on the friction layer are about 2–5 μm dimension at the velocity of 0.31 m/s whereas at the linear speed of 1.57 m/s this is about 20 μm , as shown in Fig. 8. In both of these images it can be easily seen that the abrasive particle fragmentation occurs at a high ratio especially at low speeds. This could be explained by the particle rolling time between rubbing surfaces. The high linear speed gives low rolling time and low fragmentation which leads to coarse abrasive particles. On the contrary, low linear speed gives high rolling time and high fragmentation of abrasive which leads to fine abrasive particles. It was reported that coarse abrasive particles gave high wear rate and high friction whereas fine abrasive particles give low wear and frictional properties [13]. In this study, it can be seen in Figs. 13 and 16 that there is a good agreement between the friction coefficient and wear rate for alloys. The bronze having higher friction coefficient than ZA-27 alloy with the increasing linear speed showed more high wear rate than that of ZA-27 alloy.

Figure 14 shows the relationship between wear rate and SiC% at different percentage weight ratios (3, 6, 9 and 12) in the oil. The curves obtained at 60 N applied load and at 0.31 m/s linear velocity. The wear rate of alloys increased with the increasing SiC content in the oil. The bronze showed higher ($2.3 \times 10^{-11} \text{ m}^3/\text{m}$) abrasive wear resistance than that of ZA-27 alloy ($6.29 \times 10^{-11} \text{ m}^3/\text{m}$) at the end of the test. It is well known [14] that the more amount of abrasive particles the more abrasive effect on the rubbing surface.

Friction coefficients of alloys versus sliding distance, linear velocity and applied load during tests are shown in Figs. 15, 16 and 17, respectively. As seen from Figs. 15 and 16 the friction coefficients show non-regular behaviour with the sliding distance and linear velocity. It could be attributed to the hydrodynamic interaction of oil film, random motion of the particles and particle fracture on the friction layer. On the other hand the friction decreases with the increasing applied load as clearly seen in Fig. 17. From this figure it can be seen that bronze and ZA-27 alloys

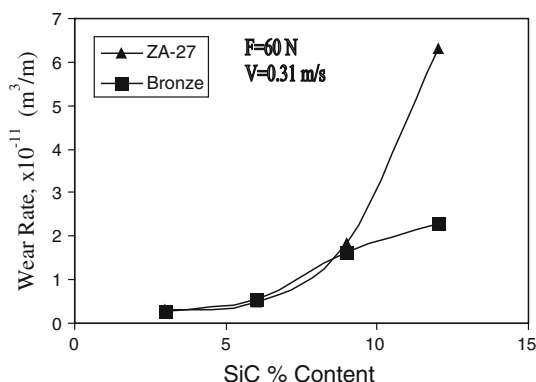


Fig. 14 Wear rate of specimens as a function of abrasive SiC content

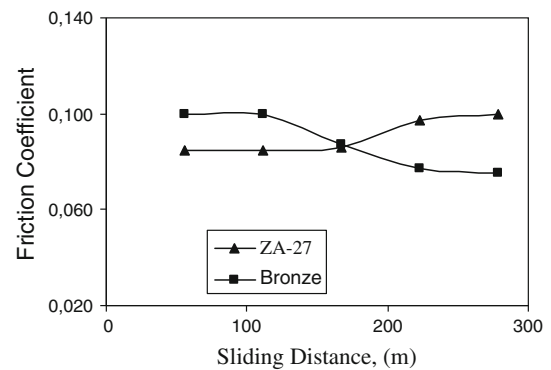


Fig. 15 Variation of friction coefficient of alloys with sliding distance

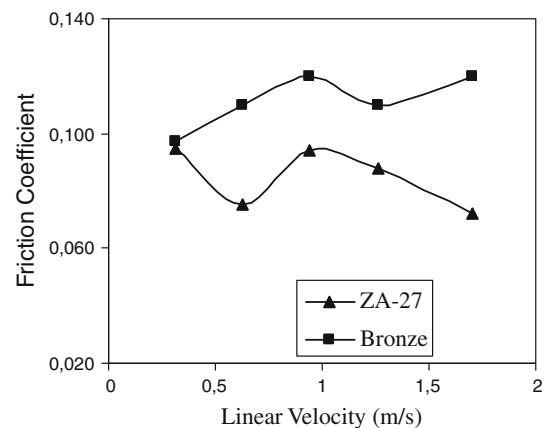


Fig. 16 Variation of friction coefficient of alloys with linear velocity

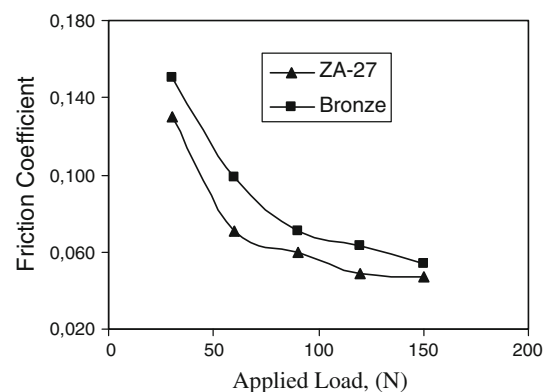


Fig. 17 Variation of friction coefficient of alloys with applied load

show similar frictional coefficient behaviour in the range of about 0.06–0.14. The coefficient of alloys shows low values such as 0.06 at the high loading conditions. This may be attributed to the more particle fracture with the increasing load. The more particle fracture leads to the more fine abrasive particles and therefore these particles give low friction coefficient data.

Friction coefficient data show low values compared to other research [9]. It solely arises due to the abrasive mixture having lubricant oil. It is well known that the lubricant oil have been used as reducing friction and wear in machine elements [15]. In addition to that the friction coefficient data as shown in Fig. 17 is good agreement with the wear rate data, Fig. 12. The friction coefficient of alloys similar to the wear rate of these decreases with increasing applied load. The decrease of friction coefficients of alloys could lead to decrease of the wear rate of alloys. This result is in good agreement with the study carried out on Zn–Al based bearings [16]. It was reported that in well-lubricated conditions the friction factors of the bearing were decreased with the increasing bearing pressure. In this study the abrasive particles added to a lubricant oil and an oil film occurs between the disc and the specimen during test which effected the wear behaviour of alloys.

The abrasive wear resistance depends on mainly the hardness of materials especially the microhardness of phases present in the alloys. In this study the macrohardnesses of material tested were found as 135 BHN for ZA-27 alloy and as 121 BHN for bronze. The bulk hardness difference between two alloys is not high and the wear resistance depends on mainly phase distribution and phase hardnesses of alloys under same testing condition. Excellent adhesive wear properties of Zn–Al alloys over bronze have been attributed to their multiphase structure and to the formation of zinc and aluminium oxides [17]. In this study ZA-27 alloy showed higher wear rate than CuSn10 bronze under abrasive test conditions. This could be explained by the formation of different friction layer and work hardening of this layer for ZA-27 alloy and CuSn10 bronze. The work hardening of different alloys having different crystal structure gives different hardness values. From this point of view copper-based bronze having mostly face centered cubic crystal structure could be more prone to work hardening than ZA-27 alloy having mostly hexagonal close-packed crystal structure. Therefore, CuSn10 showed high hardness values than ZA-27 alloy which could lead to lower wear rate than that of ZA-27.

Conclusions

The following conclusions can be drawn under the light of above results

1. CuSn10 bronze showed higher wear resistance than ZA-27 alloy under abrasive test conditions except the high linear velocities
2. Abrasive particle fracture was an important mechanism to determine friction and wear behaviour of ZA-27 alloy and CuSn10 bronze in abrasive + oil mixture condition
3. The wear rate and the friction coefficient of ZA-27 alloy and CuSn10 bronze depend on the test conditions such as linear velocity, applied load and SiC content.
4. The coarse embedded particles were found on the wear surfaces at the high linear speed such as 1.57 m/s, whereas the fine abrasive particles were present on the worn surface at the low speed such as 0.31 m/s.
5. The wear surfaces of alloys showed three distinct regions having entrance, middle and exit zones. The main wear scars were found in the middle region of the wear specimens.

Acknowledgement The authors are pleased to thank Karbosan Company for supplying abrasive particles.

References

1. Modi OP, Prasad BK, Jha AK (2006) *Wear* 260:895
2. Sarma SC, Girish BM, Kamath R, Satish BM (1998) *Wear* 219:162
3. Modi OP, Yadav RP, Mondal DP, Dasgupta R, Das S, Yegneswaran AH (2001) *J Mater Sci* 36:1601. doi:10.1023/A:1017523214073
4. Choudhury P, Das S, Datta BK (2002) *J Mater Sci* 37:2103. doi:10.1023/A:1015297904125
5. Babic M, Mitrović S, Ninković R (2009) *Tribol Ind* 31:15
6. Çuvalcı H (2001) *Turk J Eng Environ Sci* 25(3):199
7. Calayag TS (1986) 25th annual conference of metallurgists, Toronto, Ontario, pp 305–313
8. Calayag T, Ferres D (1983) Society of Automotive Engineers, Paper no. 820643
9. Dube NB, Hutchings IM (1999) *Wear* 233–235:246
10. Prasad BK (2002) *Wear* 252:250
11. Modi OP, Yadav RP, Prasad BK, Jha AK, Das S, Yegneswaran AH (2001) *Wear* 249:792
12. Al-Rubaie KS, Goldenstein H, De Mello JDB (1999) *Wear* 225–229:163
13. Pintaude G, Tanaka DK, Sinatora A (2003) *Wear* 255:55
14. Zum Gahr KH (1987) *Microstructure and wear of materials*. Elsevier Science Publishers, B.V., Netherlands
15. Bhushan B, Gupta BK (1991) *Handbook of tribology materials, coatings and surface treatments*. McGraw-Hill Inc, USA
16. Çuvalcı H, Baş H (2004) *Tribol Int* 37:433
17. Marczak RJ, Ciah R (1973) *Proceedings 1st Europe tribology congress*, London, pp 223–227